



Physiological healing of chronic gastric ulcer is not impaired by the hydrogen sulphide (H₂S)-releasing derivative of acetylsalicylic acid (ATB-340): functional and proteomic approaches

Edyta Korbut¹ · Maciej Suski^{2,3} · Zbigniew Śliwowski⁴ · Dominik Bakalarz¹ · Urszula Głowacka¹ · Dagmara Wójcik-Grzybek⁴ · Grzegorz Ginter⁴ · Kinga Krukowska¹ · Tomasz Brzozowski⁴ · Marcin Magierowski¹ · John L. Wallace⁵ · Katarzyna Magierowska⁴

Received: 23 November 2023 / Accepted: 2 March 2024
© The Author(s), under exclusive licence to Springer Nature Switzerland AG 2024

Abstract

Gastric ulcers affect approx. 10% of population. Non-steroidal anti-inflammatory drugs (NSAIDs), including acetylsalicylic acid (ASA) predispose to or impair the physiologically complex healing of pre-existing ulcers. Since H₂S is an endogenous cytoprotective molecule, we hypothesized that new H₂S-releasing ASA-derivative (ATB-340) could overcome pathological impact of NSAIDs on GI regeneration.

Clinically translational gastric ulcers were induced in Wistar rats using state-of-the-art microsurgical model employing serosal application of acetic acid. This was followed by 9 days long i.g. daily treatment with vehicle, ATB-340 (6–24 mg/kg) or equimolar ASA doses (4–14 mg/kg). Ulcer area was assessed macro- and microscopically. Prostaglandin (PG)E₂ levels, indicating pharmacological activity of NSAIDs and 8-hydroxyguanosine content, reflecting nucleic acids oxidation in serum/gastric mucosa, were determined by ELISA. Qualitative and/or quantitative pathway-specific alterations at the ulcer margin were evaluated using real-time PCR and mass spectrometry-based proteomics.

ASA, unlike ATB-340, dose-dependently delayed/impaired gastric tissue recovery, deregulating 310 proteins at the ulcer margin, including Ras signalling, wound healing or apoptosis regulators. ATB-340 maintained NSAIDs-specific cyclooxygenase-inhibiting capacity on systemic and GI level but in time-dependent manner. High dose of ATB-340 (24 mg/kg daily), but not ASA, decreased nucleic acids oxidation and upregulated anti-oxidative/anti-inflammatory heme oxygenase-1, 24-dehydrocholesterol reductase or suppressor of cytokine signalling (SOCS3) at the ulcer margin.

Thus, ASA impairs the physiological healing of pre-existing gastric ulcers, inducing the extensive molecularly functional and proteomic alterations at the wound margin. H₂S-releasing ATB-340 maintains the target activity of NSAIDs with limited impact on gastric PGE₂ signalling and physiological GI regeneration, enhancing anti-inflammatory and anti-oxidative response, and providing the pharmacological advantage.

Keywords Hydrogen sulphide · Acetylsalicylic acid · ATB-340 · Proteomics · Peptic ulcer disease · Gastric ulcer healing

✉ Katarzyna Magierowska
katarzyna.magierowska@uj.edu.pl

¹ Cellular Engineering and Isotope Diagnostics Lab, Department of Physiology, Jagiellonian University Medical College, 31-531 Krakow, Poland

² Department of Pharmacology, Jagiellonian University Medical College, Krakow, Poland

³ Proteomics Laboratory, Centre for the Development of Therapies for Civilization and Age-Related Diseases, Jagiellonian University Medical College, Krakow, Poland

⁴ Department of Physiology, Jagiellonian University Medical College, Krakow, Poland

⁵ Department of Physiology and Pharmacology, University of Calgary, Calgary, AB T2N 1N4, Canada

Introduction

Peptic ulcer disease (PUD) is an acid-dependent injury of the gastrointestinal (GI) tract that is usually located in the stomach or proximal duodenum (Malik et al. 2023). It is characterized by denuded mucosa, with the erosion extending down to the submucosa or muscularis propria (Malik et al. 2023). The estimated prevalence of peptic ulcer is approximately 10% of the global population (Kuna et al. 2019). PUD can arise due to diverse factors such as alcohol consumption, refluxed bile salts, stress, aging, and *Helicobacter pylori* infection (Fornai et al. 2011). Moreover, the predominant factors that are recognized to hinder the protective mechanisms of the gastric mucosal barrier and to predispose to PUD are non-steroidal anti-inflammatory drugs (NSAIDs) (Fornai et al. 2011). Among NSAIDs, acetylsalicylic acid (ASA), commonly known as aspirin, has been one of the most widely utilized in clinical practice, e.g., for the prevention of cardiovascular events (Fang et al. 2015). However, in line with other NSAIDs, the significant drawback of ASA lies in its adverse effects in GI tract. Even 5-aminosalicylic acid, indicated as medication of inflammatory bowel disease could cause GI side-effects (Adamowicz M et al. 2021). This pose a well-known and substantial limitation to therapeutic implementation of ASA and other NSAIDs in humans (Sostres and Lanas 2011).

However, introducing the hydrogen sulphide (H_2S)-releasing component into the structure of NSAIDs represents the new chemical approach to develop safer and even GI-repurposed derivatives of these pharmacological interventions. As a consequence, a new generation of anti-inflammatory and analgesic drugs has been designed to minimize GI toxicity. Among them, the extensively studied H_2S -releasing derivative of naproxen, ATB-346 (Otenaprexul, Antibe Therapeutics Inc.), after wide experimental investigations, has also successfully completed phase II clinical trials (Wallace and Wang 2015; Wallace et al. 2018).

H_2S , alongside nitric oxide (NO) and carbon monoxide (CO), belongs to the class of endogenous gaseous mediators and exhibits diverse and crucial physiological roles, including anti-inflammatory, vasoactive, and antioxidant properties (Farrugia and Szurszewski 2014; Wallace et al. 2015). Daily i.g. treatment with H_2S donors such as Lawesson's reagent or NaHS has been demonstrated to accelerate gastric ulcer healing in rats (Wallace et al. 2007; Magierowski et al. 2018). However, since the peptic ulcer healing is based on very complex molecular interactions (Magierowska et al. 2019), the mechanism behind the beneficial effects of H_2S -releasing compounds in this process remains incompletely understood.

Therefore, we hypothesized that new, H_2S -releasing derivative of acetylsalicylic acid (ATB-340) could provide the advantage into GI pharmacology to overcome the

toxicity of classic ASA. We sought to compare the underlying mechanisms involved in the pharmacological activity of ATB-340 vs. classic ASA, exploring the impact of chronic intragastric (i.g.) treatment with these NSAIDs on the physiological healing of pre-existing gastric ulcers. We identified pathway and target-specific alterations affected by ASA at the ulcer margin that impaired physiological tissue regeneration but could be rescued by H_2S -releasing moiety of ATB-340.

Material and methods

The experimental design and drug treatment regime

The study utilized 50 male Wistar rats aged 8–9 weeks, with an average weight ranging from 240 to 300 g. Approval for all procedures was obtained from the Institutional Animal Care and Use Committee of Jagiellonian University Medical College in Cracow, following the guidelines of the Helsinki Declaration, Directive 2010/63/EU and the replacement, refinement or reduction principle (3Rs) regarding handling of experimental animals (Decision No.: 419/2020, Date: 30 September 2020). Rats were provided with standard food and water in an appropriate environment regarding the temperature, humidity and light/dark cycle. All animal studies were performed with adherence to ARRIVE guidelines.

Prior to surgery all the animals were fasted for approx. 16 h, with free access to the water. Chronic gastric ulcers were induced based on the method originally proposed by Takagi et al. (Takagi et al. 1969) where diluted acetic acid (AA) was injected into subserosal layer. We implemented here previously described modification of this approach (Magierowski et al. 2018; Magierowska et al. 2019). Briefly, at day 0, under isoflurane anaesthesia, 40 μ L of 100% acetic acid was applied to the external, serosal part of the stomach for 25 s, using the cylinder to induce a standardized gastric necrosis (AA ulcer). Next, AA was completely removed. Therefore, this lesion morphologically developed almost immediately into a chronic ulcer, affecting the entire gastric mucosa and submucosa (Opoka et al. 2010; Magierowska et al. 2019). The healing of this experimental ulcer is similar to that clinically observed in patients suffering from peptic ulcer disease (Halter et al. 1995). Thus, one day after microsurgery, rats were randomly assigned to experimental groups ($n = 5–6$ each) and treated daily via intragastric administration (i.g.) throughout a period of subsequent 9 days with: 1) dimethyl sulfoxide (DMSO)/1% carboxymethylcellulose (CMC) solution (1:10) (vehicle), 2) ATB-340 (6, 12, 24 mg/kg), 3) ASA applied in equimolar to ATB-340 doses (4, 7, 14 mg/kg), taking into account the molecular weight of H_2S -releasing moiety (4-hydroxythiobenzamide). The

chemical structure of ATB-340 was published elsewhere (Pavlovskiy et al. 2020). Approximately 24 h after last treatment, macroscopic data and biological samples were collected, as described below. In additional experimental groups ($n=3$ each), animals were treated i.g. with vehicle, ATB-340 (24 mg/kg) or ASA (14 mg/kg). After one-hour, biological samples were collected in similar manner. The doses of H₂S-releasing derivative of NSAID (ATB-340) were selected based on previously published experimental data (Pavlovskiy et al. 2020; Głowacka et al. 2022). ATB-340 was received from Antibe Therapeutics, Inc. (Toronto, Canada). Other abovementioned chemicals were purchased from Sigma-Aldrich (Schnelldorf, Germany).

Macro- and microscopic assessment of gastric ulcer morphology

After 9 days of treatments, rats were anesthetized using pentobarbital (60 mg/kg i.p., Biowet, Pulawy, Poland). Blood samples were collected from the vena cava, centrifuged, and the serum was stored at -80°C until further analysis. Subsequently, the animals were euthanized by the administration of a lethal dose of pentobarbital. Afterward, the stomach was excised and photographed. The area of each gastric ulcer was determined blindly using planimetry and expressed in mm^2 (Magierowska et al. 2019). Gastric mucosal biopsies from the ulcer margin, not involving the muscularis mucosae, were carefully scraped off on ice. These biopsies were then snap-frozen in liquid nitrogen and stored at -80°C for subsequent assay-dependent processing and analyses (Magierowska et al. 2017).

For histological qualitative evaluation, gastric tissue sections were excised and fixed in 10% buffered formalin (pH 7.4). After dehydration through a series of alcohol concentrations and equilibration in xylene for 10–15 min, the samples were embedded in paraffin. Sections of approximately 4 μm thickness were obtained using a microtome. The resulting specimens were stained with haematoxylin/eosin (H&E) and evaluated under a light microscope (AxioVert A1, Carl Zeiss, Oberkochen, Germany). Histological slides were digitally documented using the aforementioned microscope, which was equipped with an automatic scanning table and ZEN Pro 2.3 software (Carl Zeiss, Oberkochen, Germany) (Magierowska et al. 2023). This process involved capturing multiple photographs of each histological sample and merging them into a single image.

Proteomics protocol of mass spectrometry and the data processing

Sample preparation, protein digestion and spectral library generation methodology are described in detail in (Ciszek-Lenda et al. 2023). Briefly, samples were lysed in 2% SDS,

50 mM DTT in 0.1 M Tris-HCl pH 7.6 and digested to peptides using the filter-aided sample preparation (FASP) protocol (Wiśniewski et al. 2009) with LysC-trypsin mix (Thermo Scientific, Waltham, MA, USA) at the enzyme to protein ratio 1:50. After digestion, peptide yields were determined by the tryptophan fluorescence (WF) assay (Wiśniewski and Gaugaz 2015) and aliquots containing an equal amount of total peptides were desalted in 96-Well MiniSpin C18 columns (Harvard Apparatus, Holliston, MA, USA). For project-specific spectral library preparation, an equal amount of peptides from all samples distributed across all experimental conditions was combined and subjected to the HpH fractionation protocol on C18 Micro-Spin Columns (Harvard Apparatus, Holliston, MA).

Peptides (1 μg) were injected onto a nanoEase M/Z Peptide BEH C18 75 μm i.d. \times 25 cm column (Waters, Milford, MA, USA) via a trap column nanoEase M/Z Symmetry C18 180 μm i.d. \times 2 cm column (Waters). Spectral library fractions and study samples were analysed in DDA and DIA acquisition mode, respectively. The peptides were separated using a non-linear gradient (phase A—0.1% FA; phase B—100% ACN and 0.1% FA): 0–3.5 min, 1% B; 3.5–13 min, 1–6% B; 13–60 min, 6–15% B; 60–102 min, 15–28% B; 102–115 min, 28–36% B; 115–116 min, 36–80% B; 116–126 min, 80% B; 126–126.2 min, 80–1% B; 126.2–145 min, 1% B at a flow rate of 250 nl/min by Ultimate 3000 HPLC system (Thermo Scientific, Waltham, MA, USA) and applied to an Orbitrap Exploris 480 mass spectrometer (MS) (Thermo Scientific, Waltham, MA, USA). The nano-electrospray ion source Nanospray Flex (Thermo Scientific, Waltham, MA, USA) was equipped with Simple Link Uno connector and LOTUS Sharp Singularity emitters (Fossil Ion Technology SL, Madrid, Spain). The ion spray voltage was set at 2.2 kV while the heated capillary temperature was 275 $^{\circ}\text{C}$. For DDA acquisition the mass range was set at 350–1200 m/z , the resolutions of MS1 and MS2 scans were set at 60 000 and 15 000, respectively, with a fixed cycle time (1.3 s), IT set to auto and AGC set to 500%. For DIA acquisition a survey scan of 120 000 resolution, IT set to auto and an AGC of 300% was followed by 55 DIA variable m/z segments of 15 000 resolution with IT set to auto and AGC set to 1000%. The mass range was set at 350–1650 m/z , the default charge state was set to 2 and the normalized collision energy was set to 30.

Project-specific library was generated using the rat UniProt fasta database (2023–11–01, 8 183 entries) with the criteria of 1% false discovery rate control at PSM, peptide, and protein levels, two missed cleavages and variable modifications (N-term acetylation and methionine oxidation). The latter was used to analyze the DIA data in Spectronaut 18 (Biognosys, Schlieren, Switzerland) (Bruderer et al. 2015). Data were filtered by 1% FDR on the peptide and protein level, while quantitation and interference correction were

performed on the MS2 level. Protein grouping was performed based on the ID picker algorithm (Zhang et al. 2007). Protein quantities were calculated by averaging the respective peptide intensities, while the latter were obtained as mean precursor quantities. The protein coefficients of variation (CVs) were calculated based on the summed intensities of their respective peptides. Data were normalized using a global regression strategy, while statistical testing for differential protein abundance was performed using t-tests with multiple testing correction after Storey (Storey 2002). Statistically significant differences (q value < 0.05) with quantitative cut-off for the absolute 1.5-fold change were considered as differentially regulated. The LC-MS data, library and Spectronaut project have been deposited to the ProteomeXchange Consortium via the PRIDE partner repository (Deutsch et al. 2023) with the dataset identifier PXD046894. Functional grouping and ontology/pathway annotations were performed using PINE (Sundaraman et al. 2020) and ClueGO (Bindea et al. 2009) under the Cytoscape 3.8.2 software environment (Shannon et al. 2003). KEGG (release 17.02.2020) and GO terms ontologies (release 01.11.2023) were used in the analysis. Enrichment results were validated by enrichment/depletion two-sided geometric statistical test with Bonferroni step down as p value correction method. Minimum and maximum GO levels were set as 3 and 8, respectively, with the cluster criteria of minimum 3 genes constituting a minimum of 4% of the GO term/pathway. Kappa score threshold was set at 0.4.

Determination of gastric mucosal 8-hydroxyguanosine (8-OHG) content and prostaglandin E2 (PGE2) concentration in gastric mucosa and serum

To measure 8-OHG content as an indicator of nucleic acids (RNA) oxidation, we utilized the ELISA kit (589,320, Cayman Chemical, Ann Arbor, MI, USA), following the manufacturer's protocol as described previously (Głowacka et al. 2023). Total RNA was isolated using the GeneMATRIX Universal RNA Purification Kit (EURx, Gdansk, Poland) with spin columns, adhering to the manufacturer's instructions. The 8-OHG concentration was expressed as pg of 8-OHG per 1 μ g of total RNA.

For the determination of PGE2 concentration in gastric mucosa and in serum samples, we used the PGE2 ELISA kit (ab133021, Abcam, Cambridge, UK), following the manufacturer's protocol. The homogenization process of each sample was standardized regarding sample weight and buffer volume, and results were expressed in pg/mL of gastric tissue homogenate or serum volume, as previously described (Głowacka et al. 2023).

Determination of the mRNA expression profile in gastric mucosa at the ulcer margin using real-time PCR

Gastric mucosal mRNA expression levels for cyclooxygenase (COX)-1, COX-2, superoxide dismutase 1 (SOD-1), SOD-2, glutathione peroxidase (GPx)-1, interleukin 1 β (IL-1 β), tumour necrosis factor α (TNF- α), inducible nitric oxide synthase (iNOS) and suppressor of cytokine signalling 3 (SOCS3) were determined using real-time PCR, following a previously described protocol (Magierowska et al. 2019, 2023). Briefly, succinate dehydrogenase complex, subunit A (SDHA) and β -actin (ACTB) were used as a reference genes. Total RNA was extracted from the gastric mucosa using a commercially available kit with spin-columns (GeneMATRIX Universal RNA Purification Kit, EURx, Gdansk, Poland), following the manufacturer's protocol. Reverse transcription of RNA into complementary DNA (cDNA) was performed using the High-Capacity cDNA Reverse Transcription Kit (Applied Biosystems, Foster City, CA, USA). The selected genes and their corresponding rat-specific primer sequences for real-time PCR are provided in the supplementary material (Table S1). All primers were purchased from Genomed (Warsaw, Poland).

The real-time PCR was performed using the Quant Studio 3 thermal cycler (Thermo Fisher Scientific, MA, USA) and SGqPCR Master Mix (2X) with SYBR-Green (EURx, Gdansk, Poland). Equal amounts of cDNA were added to each well to ensure consistent PCR reaction efficiency across all analyzed samples. Following the reaction, the melting curve for each sample, its technical replicates, and the appropriate negative control were examined to exclude data derived from potentially unintended products. The results were analyzed using the $-\Delta\Delta C_t$ method. Fold change of mRNA expression at ulcer margin is presented relatively to the values obtained in (healthy) intact gastric mucosal samples.

Statistical analysis and the data presentation

The experiments and data collection were conducted by operators blinded to sample identity. Analysis of the results was performed using GraphPad Prism 10 software (GraphPad Software Inc., La Jolla, CA, USA). The data are presented as mean \pm SEM. Statistical analysis employed Student's t-test or ANOVA with Bonferroni's or Dunnett's multiple comparison post hoc test when more than two experimental groups were compared. Each experimental group had mostly a sample size of $n = 5-6$, unless otherwise stated. $P < 0.05$ was considered statistically significant. Bar charts with proteomic and PCR data were drawn using group-specific white, yellow and pink columns, while functional results were additionally marked with linear patterns.

Results

Impact of ATB-340 and ASA on the physiological healing of pre-existing gastric ulcers

Figure 1A shows that daily i.g. treatment for 9 consecutive days with ATB-340 did not affect the gastric ulcer size compared to the vehicle, regardless of the dose used. This observation is in contrast with the groups treated with native NSAIDs representative, ASA. Classic ASA, applied at doses of 7 and 14 mg/kg, but not 4 mg/kg, delayed gastric ulcer healing, as reflected by the significantly increased ulcer size compared to the values observed with equivalent doses of ATB-340 (12 and 24 mg/kg, respectively) and in rats treated with the vehicle. Therefore, the doses of 14 and 24 mg/kg for ASA and ATB-340, respectively, were further analysed biochemically and molecularly.

Figure 1B shows that i.g. administration of ATB-340 (12 and 24 mg/kg daily) was associated with a decline in gastric ulcer size observed macroscopically, compared with images collected from the gastric mucosa of rats treated with corresponding doses of ASA (7 and 14 mg/kg daily). Figure 1C presents the lack of re-epithelialization

of the ulcer niche and a wide ulcer crater, reflecting representatively poor healing in the group of rats treated with ASA (14 mg/kg) compared to the vehicle and ATB-340 (24 mg/kg), where a narrower crater reflecting physiological healing and partial re-epithelialization were still observed.

Proteomic, qualitative and quantitative pathway-specific molecular alterations at ulcer margin

DDA mass spectrometry measurements for the preparation of spectral libraries resulted in the identification of 49 597 proteotypic peptides, which translated into the number of 4665 protein groups used as a DIA search matrix with Spectronaut. Spectral library precursor recovery was 89.2%, while the completeness of the protein group data was 88.6%. The median CVs of the protein groups were calculated in the range of 20.7–32.0% for all experimental groups, which allowed the estimation of a significant quantitative cut-off for an absolute 1.5-fold change (statistical power 0.9). Quantitative comparisons with the control group revealed that 151 and 310 proteins were differentially regulated in the ATB-340 (24 mg/kg) and

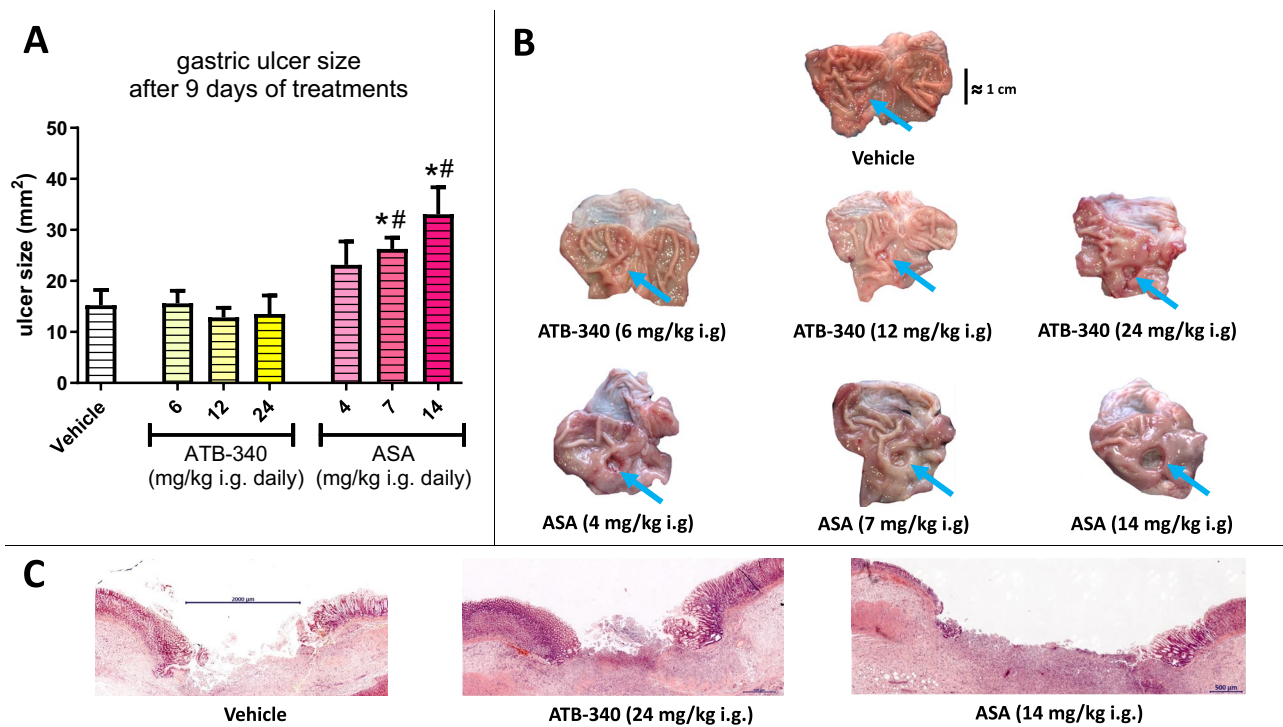


Fig. 1 The physiological healing of pre-existing gastric ulcers after the chronic treatment with ATB-340 or ASA. **(A)** Gastric ulcer size (mm²) in rats after 9 days of i.g. treatment with vehicle, ATB-340 (6, 12, 24 mg/kg daily) or ASA (4, 7, 14 mg/kg daily). Values are presented as a mean ± SEM, n = 5–6 samples per group, *p < 0.05 vs. Vehicle, #p < 0.05 vs. corresponding dose of ATB-340. **(B)** The representative macroscopic appearance of gastric mucosal ulcers, 9 days

after induction followed by the daily treatment with vehicle, ATB-340 or ASA. Blue arrows point out the gastric ulcer in each experimental group. **(C)** The microscopic representative histological slides of gastric mucosal ulcers captured 9 days after the induction that was followed by the treatment with vehicle, ATB-340 (24 mg/kg daily) or ASA (14 mg/kg daily)

ASA (14 mg/kg) groups, respectively, compared to vehicle (Supplementary Tables S2 and S3). Of note, 149 proteins were differentially regulated as directly compared ATB-340 vs ASA (Supplementary Table S4). Full list of specific targets that were affected is listed in Tables S2-S4. Importantly, most of them were functionally related to wound healing mechanisms, reactive oxygen species response and apoptosis with a clear notion that proteome-wide changes at ulcer margin were dramatically more pronounced in the ASA group compared to ATB-340 (Fig. 2A). Complete KEGG-GO enrichment analysis, including also other pathways and specific targets that were affected are listed in Supplementary Table S5.

Pharmacological efficacy of ATB-340 and ASA reflected by the altered prostaglandin (PG) E2 biosynthesis

Figure 3A illustrates the changes in PGE2 concentrations in the gastric mucosa and serum of rats with AA-induced ulcers, treated daily with vehicle, ATB-340 (24 mg/kg), and ASA (14 mg/kg) over a 9-day period (Fig. 3A, upper panel). The lower panel shows the results obtained in rats with healthy gastric mucosa (w/o AA ulcer) (Fig. 3A). Daily treatment

with ASA (14 mg/kg), but not ATB-340 (24 mg/kg), significantly reduced PGE2 content in the gastric mucosa and serum compared to vehicle-treated rats, as measured 24 h after the last application (Fig. 3A). In contrast, in rats without chronic gastric ulcer, single treatment with both ATB-340 and ASA markedly decreased mucosal and serum PGE2, 1 h after the i.g. administration (Fig. 3, lower panel). In Fig. 3B, alterations in mRNA expression of COX-1 and COX-2 in ulcerated gastric mucosa at day 9 after ulcer induction are shown. Following ulcer induction, rats were treated with vehicle, ATB-340 (24 mg/kg), and ASA (14 mg/kg). The mRNA expression of both COX-1 and COX-2 was significantly increased at the ulcer margin compared to healthy gastric mucosa (Fig. 3B). Notably, ASA led to a significant decrease in COX-1 and COX-2 mRNA expression. ATB-340 significantly reduced COX-2, but not COX-1 mRNA expression at the ulcer margin compared to vehicle (Fig. 3B). Figure 3C shows the protein levels of prostaglandin reductase1 and 2 (PTGR1 and PTGR2), and 15-hydroxyprostaglandin dehydrogenase (15-PGDH), associated with PGs inactivation and catabolism. Daily treatments with ATB-340 (24 mg/kg) and ASA (14 mg/kg) had no effect on their levels at the ulcer margin compared to vehicle-treated rats (Fig. 3C).

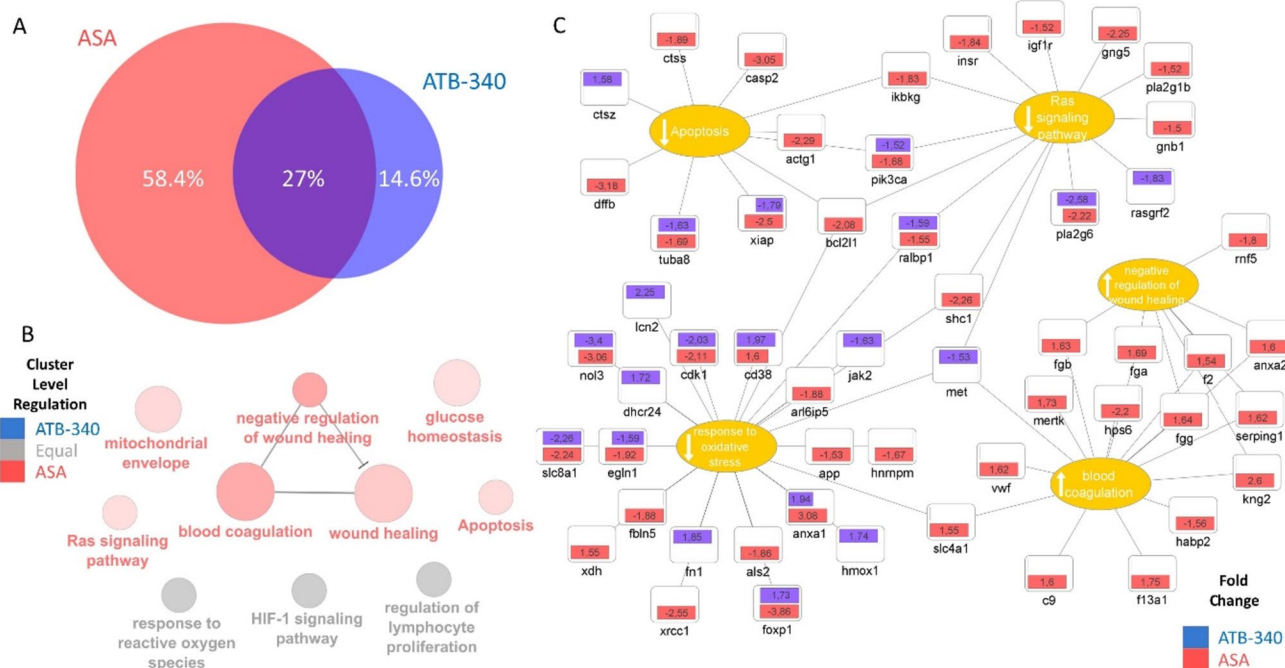


Fig. 2 Differential proteome changes elicited by ATB-340 and ASA at the margin of the gastric ulcer. **(A)** The Venn diagram showing the percentage of deregulated proteins indicates that the changes elicited by ATB-340 and ASA are qualitatively and quantitatively different, with more pronounced proteome alterations found in the ASA group. **(B-C)** Pathway-specific targets and quantitative proteomic analysis

revealing that the major differences between the examined drugs functionally enriched in clusters covering response to oxidative stress, Ras signalling, apoptosis and wound healing. The analysis evidenced that the unfavourable processes accompanying the ulcer healing are biased toward the use of ASA

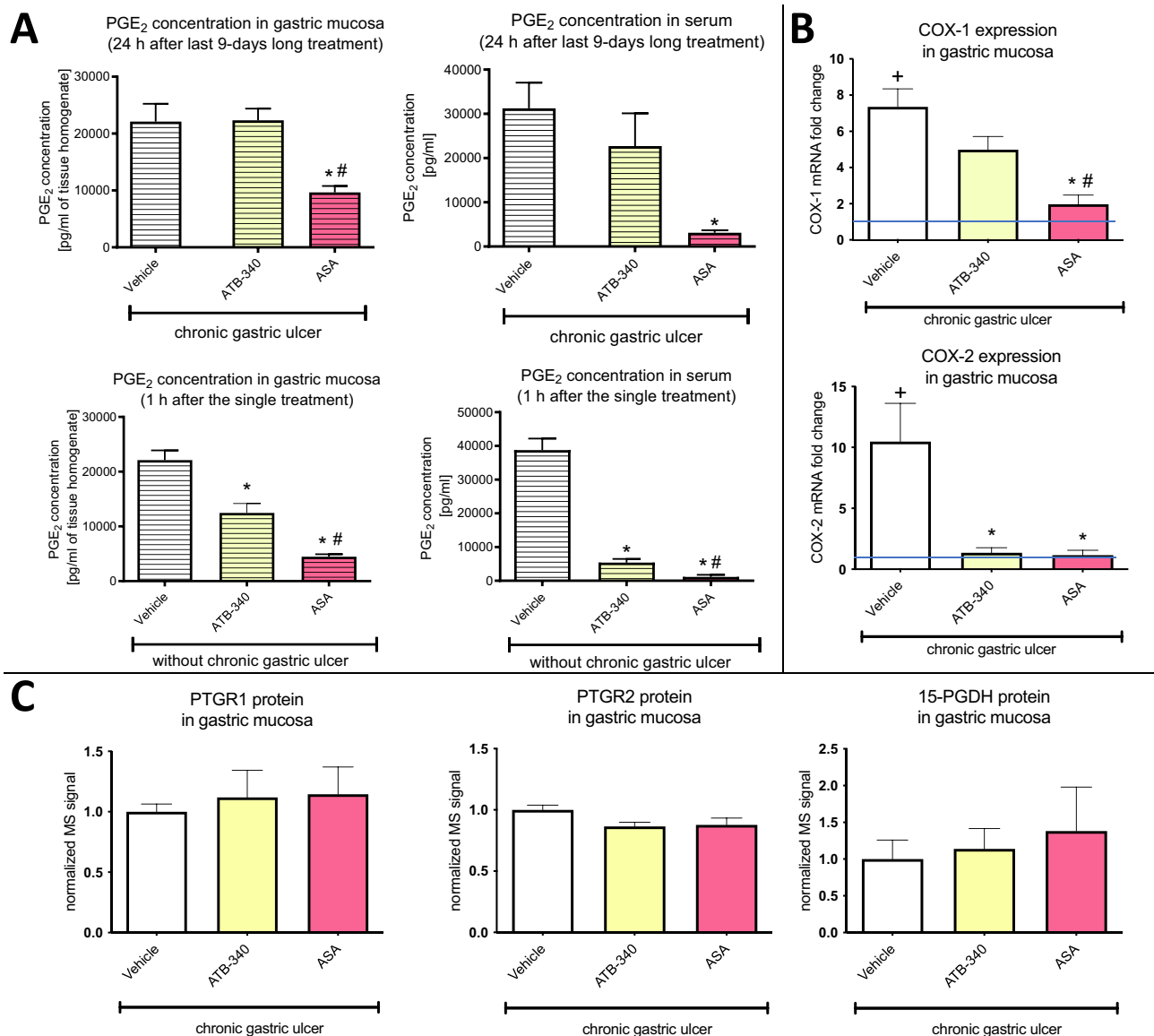


Fig. 3 Systemic and gastric mucosal alterations in prostaglandin E2 (PGE2) biosynthesis after i.g. treatment with ATB-340 or ASA. **(A)** *Upper panel*: Gastric mucosal and serum concentration of PGE2 in rats with a pre-existing AA ulcers, treated i.g. with vehicle, ATB-340 (24 mg/kg daily) and ASA (14 mg/kg daily) over a 9-days period; *Lower panel*: Gastric mucosal and serum concentration of PGE2 in rats with healthy (intact) gastric mucosa 1 h after the single i.g. application of vehicle, ATB-340 (24 mg/kg) or ASA (14 mg/kg) ($n=3$ samples per group). **(B)** mRNA expression fold change for COX-1 and COX-2 at the gastric ulcer margin of rats with a pre-existing AA

ulcer, treated i.g. with vehicle, ATB-340 (24 mg/kg daily) and ASA (14 mg/kg daily) over a 9-day period ($n=5$ samples per group). Blue line indicates baseline expression in healthy mucosa. **(C)** Normalized MS signal for PTGR1, PTGR2, and 15-PGDH protein levels at the gastric ulcer margin of rats with a pre-existing AA ulcers, treated i.g. with vehicle, ATB-340 (24 mg/kg daily) or ASA (14 mg/kg daily) over a 9-days period ($n=6$ samples per group). **(A-C)** Values are presented as a mean \pm SEM. * $p < 0.05$ vs. Vehicle, # $p < 0.05$ vs. corresponding dose of ATB-340

Impact of ATB-340 and ASA on protein levels of the enzymes involved in endogenous H₂S biosynthesis and metabolism

Figure 4A-D shows the normalized MS signal for cystathionine γ -lyase (CTH), cystathionine β -synthase (CBS), 3-mercaptopyruvate sulfurtransferase (MPST) proteins

involved in the production of H₂S, and thiosulfate sulfurtransferase (TST), which catalyzes mitochondrial H₂S clearance (Szabo et al. 2014). Daily treatment with ASA (14 mg/kg) and ATB-340 (24 mg/kg) had no effect on any of these proteins at ulcer margin compared to vehicle-treated rats.

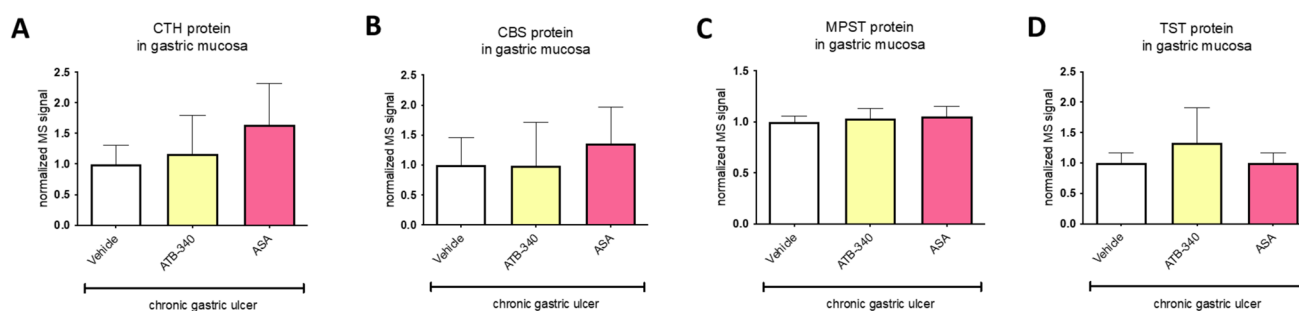


Fig. 4 Protein levels of the enzymes involved in endogenous H_2S biosynthesis and metabolism after i.g. treatment with ATB-340 or ASA. Data obtained from rats with gastric ulcers, followed by 9-days of treatments with vehicle, ATB-340 (24 mg/kg daily) or ASA (14 mg/

kg daily). Values are presented as a mean \pm SEM. (A–D) Normalized MS signal for PTGR1, PTGR2, and 15-PGDH reflecting protein levels at the gastric ulcer margin ($n=6$ samples per group).

The effect of ATB-340 and ASA on oxidative status at the ulcer margin

Figure 5A demonstrates a significant decrease in nucleic acids oxidation reflected by the concentration of 8-OHG at the gastric ulcer margin following ATB-340 (24 mg/kg), but not ASA (14 mg/kg) treatment. The gastric mRNA expression of first-line defence antioxidants, including SOD-1, SOD-2, and GPx, was significantly increased at the ulcer margin compared to healthy gastric mucosa. However, their expression levels remained unchanged following both ATB-340 and ASA treatments compared to the vehicle (Fig. 5B).

Impact of ATB-340 and ASA on mRNA expression and protein levels of selected inflammatory markers at the ulcer margin

Figure 6A illustrates the gastric mucosal mRNA expression of the pro-inflammatory cytokine IL-1 β and the protein

level of IL-1 receptor antagonist (IL-1RA). The mRNA expression of IL-1 β was significantly elevated at the ulcer margin compared to the healthy gastric mucosa, while the protein level of IL-1RA remained unchanged. Chronic treatment with either ATB-340 (24 mg/kg daily) or ASA (14 mg/kg daily) exhibited no alterations in IL-1 β expression or IL-1RA protein levels. Similarly, the mRNA expression of TNF- α , another pro-inflammatory cytokine, was significantly elevated at the ulcer margin compared to the healthy gastric mucosa. However, the protein level of TNF receptor-associated factor 6 (TRAF6) remained unchanged (Fig. 6B). Notably, in contrast to ASA, marked downregulation of TNF- α mRNA expression was observed after ATB-340 treatment compared to the vehicle (Fig. 6B). In Fig. 6C and D, the mRNA expression of the pro-inflammatory iNOS and SOCS3 was elevated at the ulcer margin compared to intact gastric mucosa. However, daily treatment with ATB-340, but not ASA, further elevated the expression of anti-inflammatory SOCS3.

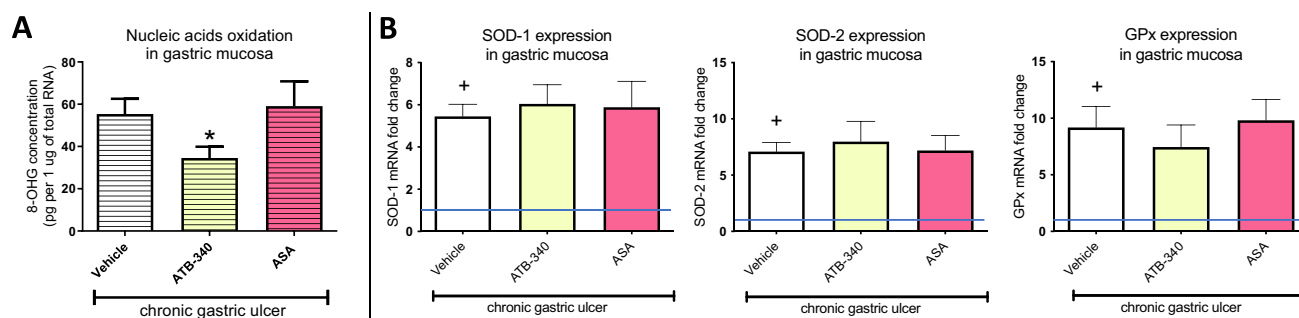


Fig. 5 Oxidative nucleic acids damage at the ulcer margin after i.g. treatment with ATB-340 or ASA. Data obtained from rats with gastric ulcers, followed by 9-days of treatments with vehicle, ATB-340 (24 mg/kg daily) or ASA (14 mg/kg daily). Values are presented as a mean \pm SEM. (A) Gastric mucosal concentration of 8-hydroxy-

guanosine (8-OHG) at the ulcer margin ($n=5$ samples per group). (B) mRNA expression for SOD-1, SOD-2 and GPx at the gastric ulcer margin ($n=5$ samples per group). Blue line indicates baseline expression in healthy mucosa. (A–D) * $p < 0.05$ vs. Vehicle, + $p < 0.05$ vs. Intact.

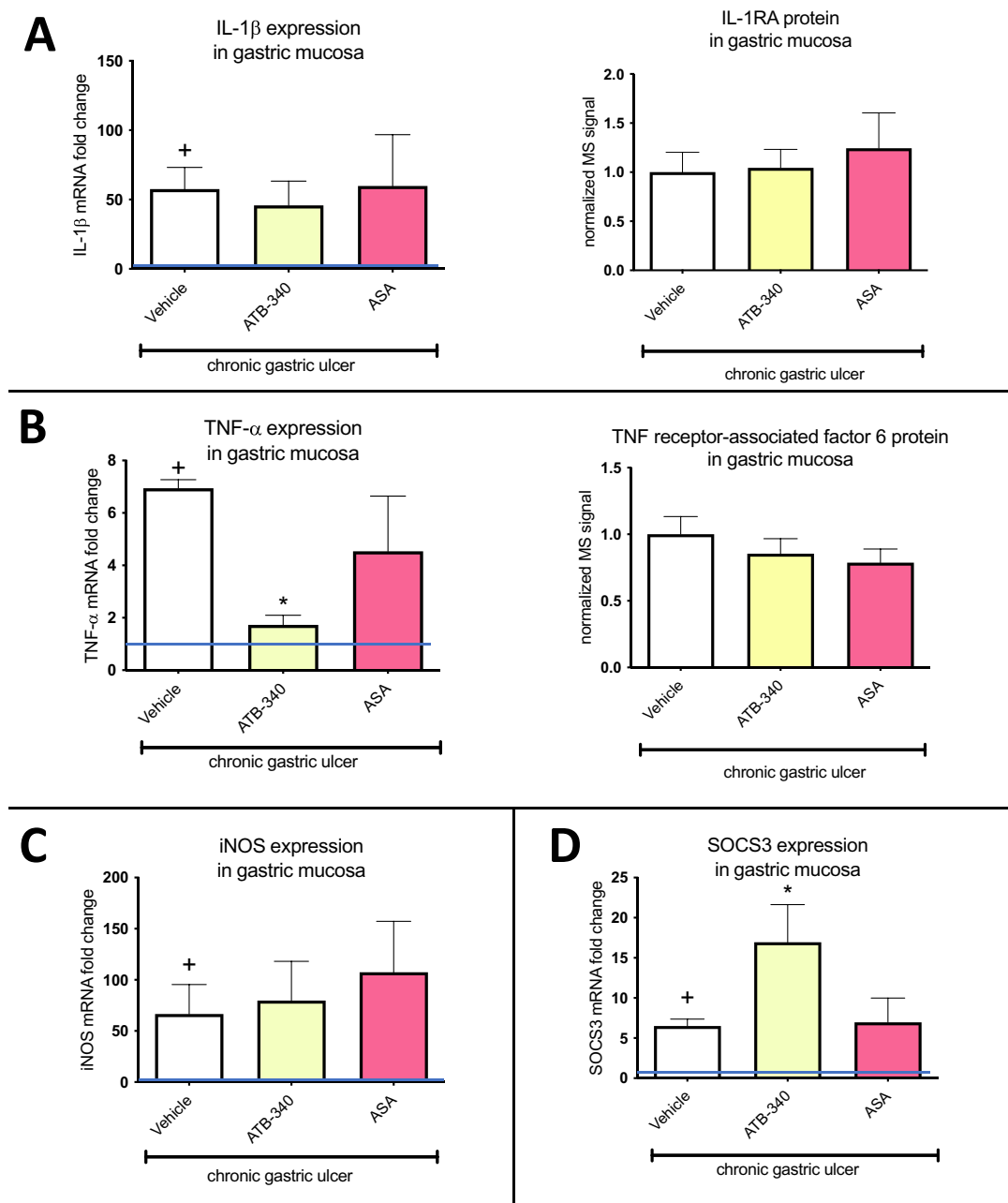


Fig. 6 Gastric mucosal mRNA expression and protein levels of selected inflammation-sensitive markers at the ulcer margin after i.g. treatment with ATB-340 or ASA. Data obtained from rats with gastric ulcers, followed by 9-days of treatments with vehicle, ATB-340 (24 mg/kg daily) or ASA (14 mg/kg daily). Values are presented as a mean \pm SEM. Blue line indicates baseline expression in healthy mucosa. (A) *Left panel*: mRNA expression for IL-1 β at the gastric ulcer margin ($n=5$ samples per group). *Right panel*: Normalized MS

signal for IL-1RA protein level ($n=6$ samples per group). (B) *Left panel*: mRNA expression for TNF- α at the gastric ulcer margin ($n=5$ samples per group). *Right panel*: Normalized MS signal for TNF receptor-associated factor 6 protein level ($n=6$ samples per group). (C) mRNA expression for iNOS at the gastric ulcer margin ($n=5$ samples per group). (D) mRNA expression for SOCS3 at the gastric ulcer margin ($n=5$ samples per group). (A-D) + $p < 0.05$ vs. Intact, * $p < 0.05$ vs. Vehicle

Discussion

Our study revealed the pharmacological advantage of the H₂S-releasing derivative of acetylsalicylic acid (ATB-340) and its ability to counteract the interference of classic

NSAIDs such as ASA into gastric mucosal integrity that limits the clinical use of these anti-inflammatories. Precisely, we observed that subsequent daily i.g. treatment with ATB-340 does not impair physiological healing of the experimental gastric ulcers. ATB-340 applied even at

high doses of 12 or 24 mg/kg was still neutral to the ulcer morphology. Whereas, equimolar concentrations of classic ASA dose-dependently delayed gastric mucosal regeneration. Simultaneously, ATB-340 exerted marginal impact on the fall in PGE2 concentration and COX-1 expression in gastric mucosa. This effect was observed only shortly after its i.g. application, in contrast to ASA affecting GI content of PGE2 even 24 h since administered. Of note, ATB-340 maintained its target pharmacological capacity to inhibit COX-1/COX-2 (reflected by PGE2 levels) on systemic level, but also in time-dependent manner. In fact, gastrotoxicity of classic ASA is evoked by the inhibition of COX-1/2-dependent PGE2 signalling that contributes to the maintenance of gastric mucosal integrity and wound healing (Pihan et al. 1986; Kolgazi M et al. 2017). Indeed, our new data revealed that in contrast to ATB-340, ASA more permanently decreased gastric mucosal PGE2 content and significantly impacted COX-1 expression at ulcer margin.

Our extensive proteomic analysis showed that in parallel with delayed ulcer healing, ASA evoked dramatic and wide-scale molecular alterations at the ulcer margin, the core of the pre-injured tissue regeneration and the starting point for the healing process. Almost 60% of deregulated proteins were specific solely to ASA treatment. On the contrary, ATB-340-associated changes at ulcer margin quantitatively covered only approx. 15% of molecular targets. Noteworthy, many of them considered as cytoprotective proteins, such as, for example, those assumed to be modulated by H₂S, anti-oxidative and inflammation-sensitive haem oxygenase 1 (HMOX-1), as well as 24-dehydrocholesterol reductase (DHCR24) (Yao et al. 2022; Głowacka et al. 2023). As a functional outcome, oxidative damage of nucleic acids at the ulcer margin was attenuated by ATB-340. This effect was not evoked by ASA which additionally downregulated the level of DNA repair protein (XRCC1). Additionally, ATB-340 decreased the expression of pro-inflammatory TNF- α and elevated anti-inflammatory SOCS3 at the ulcer margin, demonstrating its anti-inflammatory efficacy at the gastric ulcer margin.

Comparatively, ASA downregulated cell proliferation and differentiation-controlling Ras signalling that includes the arachidonic acid metabolism via phospholipase A2, group 1B (PLA2G1B). This phenomenon could indirectly contribute to the above mentioned fall in the biosynthesis of PGs. Our data showed that ASA also impeded the apoptosis, e.g., via downregulation of caspase-2 (CASP2) or cathepsin S (CTSS) proteins. Most importantly, ASA-evoked molecular turnover at the ulcer margin resulted in the upregulation of the negative regulators of wound healing, such as serpin family G member 1 (SERPING1), annexin A2 (ANXA2), fibrinogen alpha chain (FGA) or RING finger protein 5 (RNF5). At subcellular level, we

showed that ASA, but not ATB-340, deregulated strongly mitochondrial envelope cluster. This data are in line with our recent study where we observed that i.g. pretreatment with mitochondria-targeted H₂S donor (AP39) restored mitochondrial capacity to counteract ASA-induced redox imbalance in gastric mucosa (Magierowska et al. 2023). ATB-340 is not a targeted H₂S donor but our new data confirm that its antioxidative and H₂S-releasing ability could be mechanistically due to the maintenance of proteomic balance in mitochondria, considered as a crucial organelle for H₂S signalling and H₂S-therapeutics (Szabo et al. 2014; Gilbert and Pluth 2022).

Previous studies showed that endogenous H₂S and H₂S-donors not only prevented gastric mucosa damage, but also accelerated pre-existing gastric ulcers healing (Wallace et al. 2007; Magierowski et al. 2018). These data confirmed the therapeutic properties of this gaseous molecule that could be implied in GI pharmacology. Our new findings do not show any alterations at the ulcer margin regarding protein levels of the enzymes involved in endogenous H₂S metabolism. Therefore, biological effects were due to the activity of H₂S released from the chemical moiety of ATB-340.

Taken together, we conclude that H₂S-releasing capacity of ATB-340 maintains the target pharmacological activity of NSAIDs in time-dependent manner but additionally provides the evident advantage over classic ASA, counteracting its gastric toxicity and negative impact on GI regeneration. In contrary, ASA impairs the physiological healing of pre-existing gastric ulcers, inducing the extensive molecular functional and proteomic shift at the ulcer margin. However, chronic i.g. treatment, even with high doses of H₂S-donating ATB-340 is morphologically and molecularly more neutral to complex physiological regenerative processes within GI tract. ATB-340 additionally enhances anti-inflammatory and anti-oxidative response providing a new approach into the NSAIDs-based GI pharmacology.

Supplementary Information The online version contains supplementary material available at <https://doi.org/10.1007/s10787-024-01458-3>.

Acknowledgements We would like to thank to Anna Chmura, MSc (Department of Physiology, Jagiellonian University Medical College, Krakow, Poland) for technical processing of histological slides and to Malgorzata Szetela, MSc (Cellular Engineering and Isotope Diagnostics Lab, Department of Physiology, Jagiellonian University Medical College, Krakow, Poland) for her technical assistance covering samples processing for biochemical and molecular assays.

Authors contributions Conceptualization: K.M.; Funding acquisition: K.M.; Investigation/Experiments (in vivo): Z.S., M.M., D.W.G., G.G., T.B., K.M.; Biochemical and Molecular Investigation/Experiments: E.K., M.S., U.G., D.B., K.K., K.M.; Methodology: E.K., K.M.; Methodology (proteomics): M.S.; Resources: J.L.W., K.M.; Supervision: M.M., K.M.; Visualization: E.K., M.S., K.M.; Writing—original draft: E.K., K.M.; Writing—review & editing: M.S., M.M., K.M.; All authors have read and agreed to this version of the manuscript.

Funding This study was supported by statutory grants for K.M. (N41/DBS/000877, N41/DBS/000578) received from Jagiellonian University Medical College (Krakow, Poland). Part of the molecular studies were supported by the grant from The National Centre for Research and Development, Poland (LIDER/ 9/0055/L-8/16/NCBR/2017). The proteomics study was carried out with the use of research infrastructure co-financed by the Smart Growth Operational Programme POIR 4.2 project no. POIR.04.02.00–00-D023/20.

Data availability Additional data and methodological details are attached as Supplementary Materials. Any other supportive data available upon reasonable request to corresponding author. The mass spectrometry proteomics data have been deposited to the ProteomeXchange Consortium via the PRIDE partner repository with the dataset identifier PXD046894.

Declarations

Conflicts of interest J.L.W. is a co-founder of Antibe Therapeutics Inc. Other authors have nothing to disclose.

References

- Adamowicz M, Milkiewicz P, Kempinska-Podhorodecka A (2021) 5-aminosalicylic acid inhibits the expression of oncomiRs and pro-inflammatory microRNAs: an in vitro study. *J Physiol Pharmacol* 72(4):529–535. <https://doi.org/10.26402/jpp.2021.4.04>
- Bindea G, Mlecnik B, Hackl H et al (2009) ClueGO: a Cytoscape plugin to decipher functionally grouped gene ontology and pathway annotation networks. *Bioinformatics* 25:1091–1093. <https://doi.org/10.1093/BIOINFORMATICS/BTP101>
- Bruderer R, Bernhardt OM, Gandhi T et al (2015) Extending the limits of quantitative proteome profiling with data-independent acquisition and application to acetaminophen-treated three-dimensional liver microtissues. *Mol Cell Proteomics* 14:1400–1410. <https://doi.org/10.1074/MCP.M114.044305>
- Ciszek-Lenda M, Majka G, Suski M et al (2023) Biofilm-forming strains of *P. aeruginosa* and *S. aureus* isolated from cystic fibrosis patients differently affect inflammatory phenotype of macrophages. *Inflamm Res* 72:1275. <https://doi.org/10.1007/S00011-023-01743-X>
- Deutsch EW, Bandeira N, Perez-Riverol Y et al (2023) The ProteomeXchange consortium at 10 years: 2023 update. *Nucleic Acids Res* 51:D1539. <https://doi.org/10.1093/NAR/GKAC1040>
- Fang J, George MG, Gindi RM et al (2015) Use of low-dose aspirin as secondary prevention of atherosclerotic cardiovascular disease in US Adults (from the National Health Interview Survey, 2012). *Am J Cardiol* 115:895–900. <https://doi.org/10.1016/J.AMJCA.RD.2015.01.014>
- Farrugia G, Szurszewski JH (2014) Carbon monoxide, hydrogen sulfide, and nitric oxide as signaling molecules in the gastrointestinal tract. *Gastroenterology* 147:303–313. <https://doi.org/10.1053/J.GASTRO.2014.04.041>
- Fornai M, Antonioli L, Colucci R et al (2011) Pathophysiology of gastric ulcer development and healing: molecular mechanisms and novel therapeutic options. *Peptic Ulcer Dis*. <https://doi.org/10.5772/17640>
- Gilbert AK, Pluth MD (2022) Subcellular delivery of hydrogen sulfide using small molecule donors impacts organelle stress. *J Am Chem Soc* 144:17651–17660. <https://doi.org/10.1021/JACS.2C07225>
- Głowacka U, Magierowska K, Wójcik D et al (2022) Microbiome profile and molecular pathways alterations in gastrointestinal tract by hydrogen sulfide-releasing nonsteroidal anti-inflammatory drug (ATB-352): insight into possible safer polypharmacy. *Antioxid Redox Signal* 36:189–210. <https://doi.org/10.1089/ARS.2020.8240>
- Głowacka U, Magierowski M, Śliwowski Z et al (2023) Hydrogen sulfide-releasing indomethacin-derivative (ATB-344) prevents the development of oxidative gastric mucosal injuries. *Antioxidants*. 12:1545
- Halter F, Schmassmann A, Tarnawski A (1995) Healing of experimental gastric ulcers - Interference by gastric acid. *Dig Dis Sci* 40:2481–2486. <https://doi.org/10.1007/BF02063260/METRICS>
- Kolgazi M, Ozdemir-Kumral ZN, Cantali-Ozturk C et al (2017) Anti-inflammatory effects of nesfatin-1 on acetic acid-induced gastric ulcer in rats: involvement of cyclo-oxygenase pathway. *J Physiol Pharmacol* 68:756–777
- Kuna L, Jakab J, Smolic R et al (2019) Peptic ulcer disease: a brief review of conventional therapy and herbal treatment options. *J Clin Med* 8:179. <https://doi.org/10.3390/JCM8020179>
- Magierowska K, Bakalarz D, Wójcik D et al (2019) Time-dependent course of gastric ulcer healing and molecular markers profile modulated by increased gastric mucosal content of carbon monoxide released from its pharmacological donor. *Biochem Pharmacol* 163:71–83. <https://doi.org/10.1016/j.bcp.2019.02.011>
- Magierowska K, Wójcik-Grzybek D, Korbut E et al (2023) The mitochondria-targeted sulfide delivery molecule attenuates drug-induced gastropathy. Involvement of heme oxygenase pathway. *Redox Biol* 66:102847. <https://doi.org/10.1016/J.REDOX.2023.102847>
- Magierowski M, Magierowska K, Hubalewska-Mazgaj M, Sliwowski Z, Pajdo R, Ginter G, Kwiecien S, Brzozowski T (2017) Exogenous and endogenous hydrogen sulfide protects gastric mucosa against the formation and time-dependent development of ischemia/reperfusion-induced acute lesions progressing into deeper ulcerations. *Molecules* 22(2):295. <https://doi.org/10.3390/molecules22020295>
- Magierowski M, Magierowska K, Hubalewska-Mazgaj M et al (2018) Cross-talk between hydrogen sulfide and carbon monoxide in the mechanism of experimental gastric ulcers healing, regulation of gastric blood flow and accompanying inflammation. *Biochem Pharmacol* 149:131–142. <https://doi.org/10.1016/J.BCP.2017.11.020>
- Malik TF, Gnanapandithan K, Singh K (2023) Peptic Ulcer Disease. *Sex/Gender-Specific Medicine in the Gastrointestinal Diseases* 131–151. Doi: https://doi.org/10.1007/978-981-19-0120-1_9
- Opoka W, Adamek D, Plonka M et al (2010) Importance of luminal and mucosal zinc in the mechanism of experimental gastric ulcer healing. *J Physiol Pharmacol* 61:581–591
- Pavlovskiy Y, Yashchenko A, Zayachkivska O (2020) H2S donors reverse age-related gastric malfunction impaired due to fructose-induced injury via CBS, CSE, and TST expression. *Front Pharmacol* 11:558245
- Pihan G, Majzoubi D, Haudenschild C et al (1986) Early microcirculatory stasis in acute gastric mucosal injury in the rat and prevention by 16,16-dimethyl prostaglandin E2 or sodium thiosulfate. *Gastroenterology* 91:1415–1426. [https://doi.org/10.1016/0016-5085\(86\)90195-2](https://doi.org/10.1016/0016-5085(86)90195-2)
- Shannon P, Markiel A, Ozier O et al (2003) Cytoscape: a software environment for integrated models of biomolecular interaction networks. *Genome Res* 13:2498. <https://doi.org/10.1101/GR.1239303>
- Sostres C, Lanás A (2011) Gastrointestinal effects of aspirin. *Nat Rev Gastroenterol Hepatol* 8(7):385–394. <https://doi.org/10.1038/nrgastro.2011.97>
- Storey JD (2002) A direct approach to false discovery rates. *J R Stat Soc Series B Stat Methodol* 64:479–498. <https://doi.org/10.1111/1467-9868.00346>

- Sundaraman N, Go J, Robinson AE et al (2020) PINE: an automation tool to extract and visualize protein-centric functional networks. *J Am Soc Mass Spectrom* 31:1410–1421. <https://doi.org/10.1021/JASMS.0C00032>
- Szabo C, Ransy C, Módos K et al (2014) Regulation of mitochondrial bioenergetic function by hydrogen sulfide. Part I. Biochemical and physiological mechanisms. *Br J Pharmacol* 171:2099–2122. <https://doi.org/10.1111/bph.12369>
- Takagi K, Okabe S, Saziki R (1969) A new method for the production of chronic gastric ulcer in rats and the effect of several drugs on its healing. *Jpn J Pharmacol* 19:418–426. <https://doi.org/10.1254/jjp.19.418>
- Wallace JL, Wang R (2015) Hydrogen sulfide-based therapeutics: exploiting a unique but ubiquitous gasotransmitter. *Nat Rev Drug Discov* 14(5):329–345. <https://doi.org/10.1038/nrd4433>
- Wallace JL, Dickey M, McKnight W, Martin GR (2007) Hydrogen sulfide enhances ulcer healing in rats. *FASEB J* 21:4070–4076. <https://doi.org/10.1096/FJ.07-8669COM>
- Wallace JL, Blackler RW, Chan MV et al (2015) Anti-inflammatory and cytoprotective actions of hydrogen sulfide: translation to therapeutics. *Antioxid Redox Signal* 22:398–410. <https://doi.org/10.1089/ARS.2014.5901>
- Wallace JL, Vaughan D, Dickey M et al (2018) Hydrogen sulfide-releasing therapeutics: translation to the clinic. *Antioxid Redox Signal* 28:1533–1540. <https://doi.org/10.1089/ARS.2017.7068>
- Wiśniewski JR, Zougman A, Nagaraj N, Mann M (2009) Universal sample preparation method for proteome analysis. *Nat Methods* 6(5):359–362
- Wisniewski JR, Gaugaz FZ (2015) Fast and sensitive total protein and peptide assays for proteomic analysis. *Anal Chem* 87:4110–4116. https://doi.org/10.1021/AC504689Z/ASSET/IMAGES/LARGE/AC-2014-04689Z_0006.JPEG
- Yao M, Li F, Xu L et al (2022) 24-Dehydrocholesterol Reductase alleviates oxidative damage-induced apoptosis in alveolar epithelial cells via regulating Phosphatidylinositol-3-Kinase/Protein Kinase B activation. *Bioengineered* 13:155–163. <https://doi.org/10.1080/21655979.2021.2011634>
- Zhang B, Chambers MC, Tabb DL (2007) Proteomic parsimony through bipartite graph analysis improves accuracy and transparency. *J Proteome Res* 6:3549–3557. <https://doi.org/10.1021/PR070230D>

Publisher's Note Springer Nature remains neutral with regard to jurisdictional claims in published maps and institutional affiliations.

Springer Nature or its licensor (e.g. a society or other partner) holds exclusive rights to this article under a publishing agreement with the author(s) or other rightsholder(s); author self-archiving of the accepted manuscript version of this article is solely governed by the terms of such publishing agreement and applicable law.